Biodiesel obtained by ethylic transesterification using CuO, ZnO and CeO$_2$ supported on bentonite

Ana Flávia F. Farias [a], Kleber F. Moura [a], Juliana K.D. Souza [a], Regineide O. Lima [b], Jakeline D.S.S. Nascimento [c], Adriana A. Cutrim [d], Elson Longo [e], Antônio S. Araujo [b], José Rodrigues Carvalho-Filho [a], Antonio G. Souza [a], Ieda M.G. Santos [a,*]

[a] LACOM/INCTMN, Universidade Federal da Paraíba, João Pessoa, PB, Brazil
[b] Universidade Federal do Rio Grande do Norte, Natal, RN, Brazil
[c] CPTECH Bentonisa, Bentonita do Nordeste, S.A. João Pessoa, PB, Brazil
[d] Universidade Federal de Campina Grande, Campina Grande, PB, Brazil
[e] LIEC/INCTMN, Instituto de Química, UNESP, Araraquara, SP, Brazil

HIGHLIGHTS

- Montmorillonite was impregnated with different oxides for biodiesel synthesis.
- Biodiesel was obtained by ethylic transesterification, while most papers use the methylic one.
- More than 80% conversion was obtained in a green chemistry process using ZnO impregnated on natural bentonite.

GRAPHICAL ABSTRACT
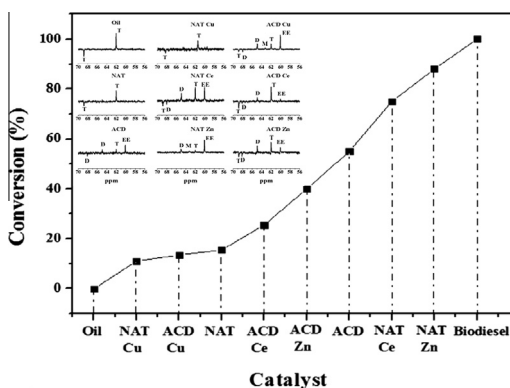
ARTICLE INFO

ABSTRACT

This research aims to study the feasibility of using bentonite clays in their natural form, acidified and impregnated with CuO, ZnO and CeO$_2$ by a microwave-assisted solvothermal method, for use in the production of biodiesel. Characterization of the materials confirmed impregnation on the bentonite. Transesterification reactions were performed using the ethylic route at 200 °C in a Parr reactor for 1, 2 and 4 h. The results indicated that acidified bentonite led to the conversion of triacylglycerides into esters in addition to small amounts of diacylglycerides and monoacylglycerides. However, this material does not lead to the homogeneous impregnation of the oxides on its surface. For the natural bentonite, almost no conversion was obtained for the pure material, but a homogeneous impregnation with zinc oxide was attained, leading to 88% conversion after 4 h of a catalytic test.

© 2015 Elsevier Ltd. All rights reserved.

1. Introduction

Natural clays have been used in catalytic reactions. For instance, K-10 montmorillonite and HB zeolite were used as catalysts in the

* Corresponding author.
  E-mail address: ieda@quimica.ufpb.br (I.M.G. Santos).

methylic transesterification of *Pongamia pinnata* oil at 120 °C for 24 h. Conversions of 47% and 59% were obtained, respectively [1,2].

The structural properties of clay minerals can be modified by different methods or can be used as supports for the deposition of catalysts. The use of a catalytic support aims to increase the surface area and improve the dispersion of the active phase leading to more active sites [2,3]. In the present work, a bentonite was used as a support for ZnO, CuO and CeO$_2$.

ZnO is a material with promising results in the synthesis of biodiesel, with conversions up to 96% depending on the method of synthesis and the reaction conditions during transesterification [4]. Karmee and Chadha [1] obtained an 83% conversion in the methylic transesterification of *Pongamia pinnata* oil at 120 °C for 24 h. The simultaneous synthesis of nanometric ZnO and biodiesel was performed by the solvothermal reaction of vegetable oils and zinc nitrate in methanolic media with conversion of almost 97% [5]. Zinc was also used as a salt for the methanolic transesterification of castor oil [6,7]. ZnO was also mixed with other oxides, as CaO, La$_2$O$_3$ or SiO$_2$ for the transesterification reaction [8–12].

CuO has been mixed with other oxides and used in the synthesis of biodiesel from cooking oil. CuO–CeO$_2$ mixed oxides led to 92% conversion [13]. Caland et al. [14] obtained ~84% conversion using CuO–Al$_2$O$_3$ for the methanolic transesterification of babassu oil. CuO was supported on SrO for the transesterification reaction in addition to the selective hydrogenation of hempseed oil [15].

CeO$_2$ has been used as a support or mixed with other oxides for the methanolic transesterification of different oils. For instance, CeO$_2$–CaO mixed oxides were used as catalysts by Thitsartarn and Kawi [16] for the methanolic transesterification of palm oil with 95% conversion and also by Kawashima et al. [17], with 80% conversion. Ramírez et al. [18] obtained 56% conversion after 1 h of reaction for CeO$_2$ impregnated on MgO in the transesterification of cooking oil. In other studies, CeO$_2$ was used as a support for CaO in the methylic transesterification of soybean oil. [19,20].

In the present work, ZnO, CuO and CeO$_2$ were deposited on bentonite using the microwave-assisted hydrothermal/solvothermal method of synthesis, which has been widely used to obtain nanometric materials with different compositions [21]. The transesterification reaction was performed by the ethylic route because Brazil produces ethanol from sugar cane, which leads to a very green fuel.

2. Materials and methods

2.1. Synthesis of the catalytic system

The natural (NAT) and acid (ACD) clays were provided by BETONISA S.A. ZnO and CuO solutions were prepared separately using acetates as precursors (Zn$_2$(CH$_3$COO)$_2$·H$_2$O and Cu (CH$_3$COO)$_2$·H$_2$O, respectively) under ethanolic media and CeO$_2$ was obtained using Ce(SO$_4$)$_2$·4H$_2$O in aqueous media. All of the suspensions were obtained after alkalinization by NH$_4$OH. The bentonite was added to the suspension containing the cations under constant stirring for 20 min and solvothermalized/hydrothermalized in a microwave reactor at 100 °C for 15 min. The precipitated material was washed with distilled water in a centrifuge until neutralization at pH = 7 and dried at 100 °C for 5 h. Samples were named based on the bentonite used as the support (NAT for the natural one and ACD for the acid one) and the symbol of the cation present in each oxide.

Powders were characterized by X-ray diffraction in an XRD 6000 instrument from Shimadzu using K$_\alpha$ (Cu) radiation (λ = 1.54), a step scan of 0.03°/s and a 2θ range of 3–80°. Analyses of the surface area were performed by N$_2$ adsorption using the BET equation. Measurements were taken in a BELSORP

II instrument. FE-SEM micrographs were performed using a FEG-VP Zeiss Supra 35 instrument.

For the catalysts NAT, ACD, NAT Zn and ACD Zn, the acid sites were determined by the n-butylamine adsorption/desorption, according to the methodology described by Silva et al. [22], except for the activation temperature which was done at 200 °C instead of 400 °C, due to the clay dehydroxylation reaction which takes place between 400 and 500 °C. Quantification of the n-butylamine adsorbed/chemisorbed on the acid sites was performed by thermosorption using thermogravimetry measurements by a Mettler 851 TG/SDTA equipment. For this calculation the mass loss assigned to dehydroxylation was subtracted from the total mass loss. The analyses were carried out in alumina crucibles containing ca. 10 mg of sample pre-adsorbed with n-butylamine. High purity nitrogen was used as carrier gas was with a flow of 25 mL min^{-1}. Samples were heated with a rate of 10 °C min^{-1} up to 850 °C.

2.2. Catalytic test

Synthesis of the biodiesel was performed using ethyl alcohol and soybean oil in a molar ratio of 12:1. The catalysts were used in a concentration of 5% m/m. Reactions were performed in a Parr reactor, model 4561, with a capacity of 300 mL. The reagents were placed in the reactor and heated to 200 °C at a heating rate of 2 °C min^{-1} under stirring at a speed of 600 rpm. The final pressure varied from 300 to 330 psi. Samples of 35 mL were removed from the reactor after 1, 2 and 4 h. These samples were centrifuged for separation of the catalysts and then transferred to a decantation balloon, where they were washed and dried at 80 °C under vacuum.

The biodiesel samples were characterized by kinematic viscosity measurements using a Julab viscometer, model V18, with a Cannon Fenske glass capillary immersed in a water bath at 40 °C. ^{1}H NMR spectra were obtained on a GEMINI 300BB VARIAN spectrometer operating at a frequency of 200 MHz. Conversion of the oil into biodiesel was evaluated based on the integrated peaks of the spectra [23–25] according to the methodology developed by Ghesti [24]. The concentration of the ethylic esters was determined using a gas chromatograph with a flame ionizing detector (GC-FID) from Shimadzu, model CGMS-2010, with an automatic sampler and a split injector. The capillary column Durabond – DB-23 (Agilent Technologies) was used. Helium was used as the carrier gas with a flow rate of 30.0 mL min^{-1} and an injection volume of 0.5 µL. The temperature of the FID detector was 380 °C.

3. Results and discussion

3.1. Synthesis of the catalysts

The XRD patterns of the pure and impregnated bentonites are presented in Fig. 1 and Table 1. The presence of smectite was confirmed, in addition to quartz and minor amounts of illite and kaolinite. One peak assigned to CeO$_2$ was identified at 28°, which confirmed the formation of the fluorite phase. Superposition of the peaks assigned to CuO and ZnO with those of the smectite made identification of these phases difficult. Moreover, this behavior may be related to the formation of ZnO and CuO with low crystallinity, which would lead to low-intensity peaks in the XRD patterns.

After deposition of the oxide on the bentonite, a significant decrease in the intensity of the (0 0 1) peak of the smectite can be observed, in addition to its dislocation to larger angles, which indicate that the interlamellar distance decreased. This behavior can be assigned to the intercalation of H$_3$O$^+$ molecules among the lamellae being exchanged with hydrated Na$^+$ cations.
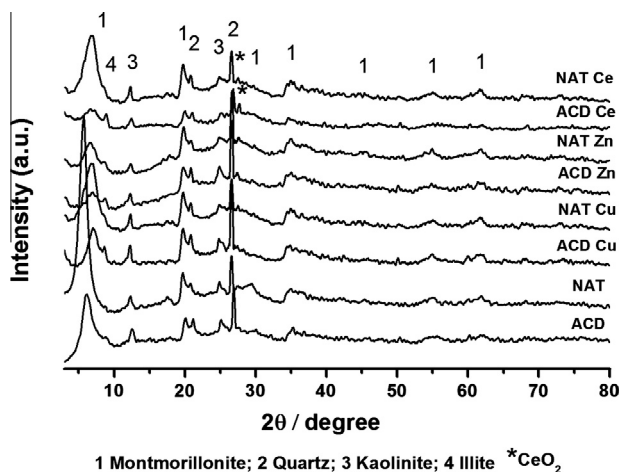
Fig. 1. XRD patterns of the natural (NAT) and acidified (ACD) clays impregnated with CuO, ZnO and CeO$_2$.

Table 1
Results obtained by XRD and N$_2$ adsorption measurements.

Catalyst	2θ Angle (°)	d_{001} (Å)	S_{BET} (m^2/g)
NAT	5.7	15.4	54
NAT Cu	6.8	12.9	54
NAT Ce	6.8	12.9	120
NAT Zn	6.6	13.4	64
ACD	6.1	14.4	15
ACD Cu	7.0	12.6	56
ACD Ce	6.6	13.3	94
ACD Zn	7.0	12.7	58

For the systems composed of oxides deposited on natural bentonite, changes were similar to those observed for the acid bentonite. The decrease in the interlamellar distance indicates that these oxides are deposited not only on the surface of the smectite but also among the lamellae. For the samples obtained from deposition of the oxides on the acid clay, a decrease in the intensity of the (001) peaks and a shift to larger angles was also observed.

The results related to the $d_{(001)}$ values obtained in the present work are similar to the literature data concerning natural montmorillonite and in relation to the dislocation of the (001) peaks when clays are acidified or impregnated with metals [3,26,27].

Evaluation of the morphology was performed by FE-SEM, as shown in Fig. 2. Micrographs of the bentonite samples impregnated with CuO, ZnO and CeO$_2$ showed the dispersion of the metal oxides on the clay. For the acid bentonite, the formation of agglomerates on and beside the clay particles was observed. As these images were obtained with a backscattering signal, brighter regions are related to atoms with larger atomic numbers, as clearly observed for the ACD Ce sample. When impregnation was
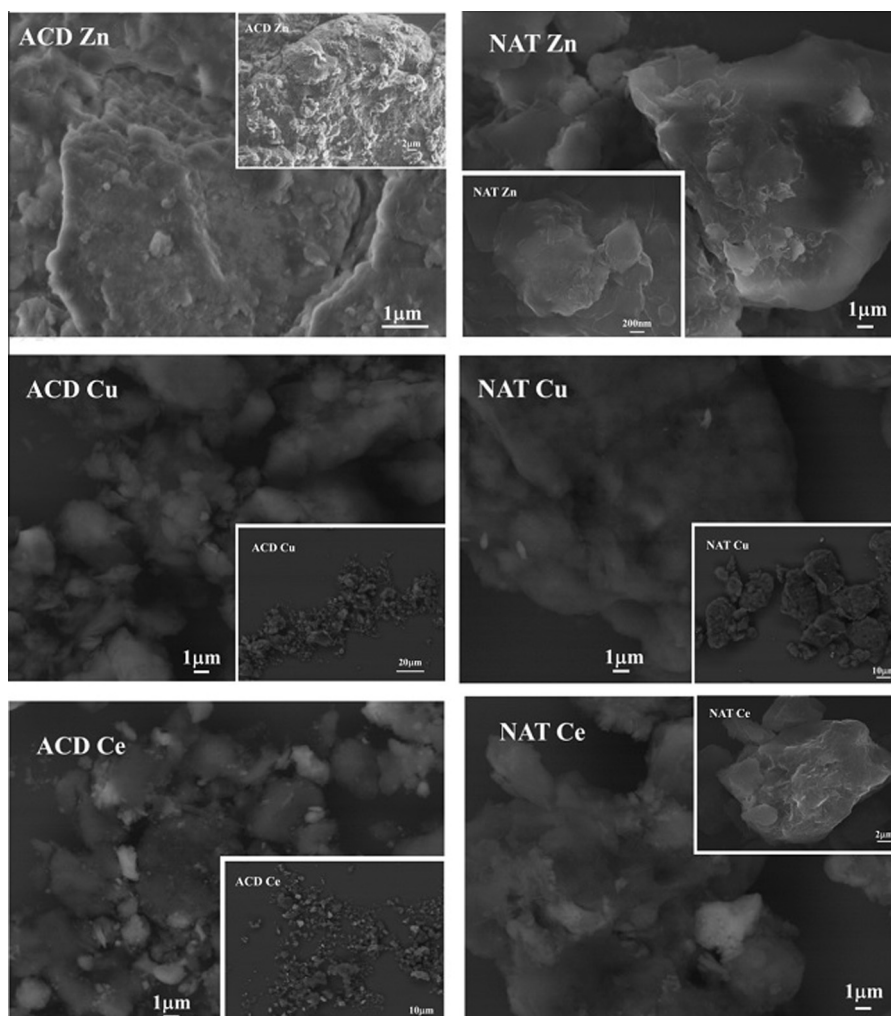

Fig. 2. FE-SEM images of the bentonite samples impregnated with CuO, ZnO or CeO$_2$.
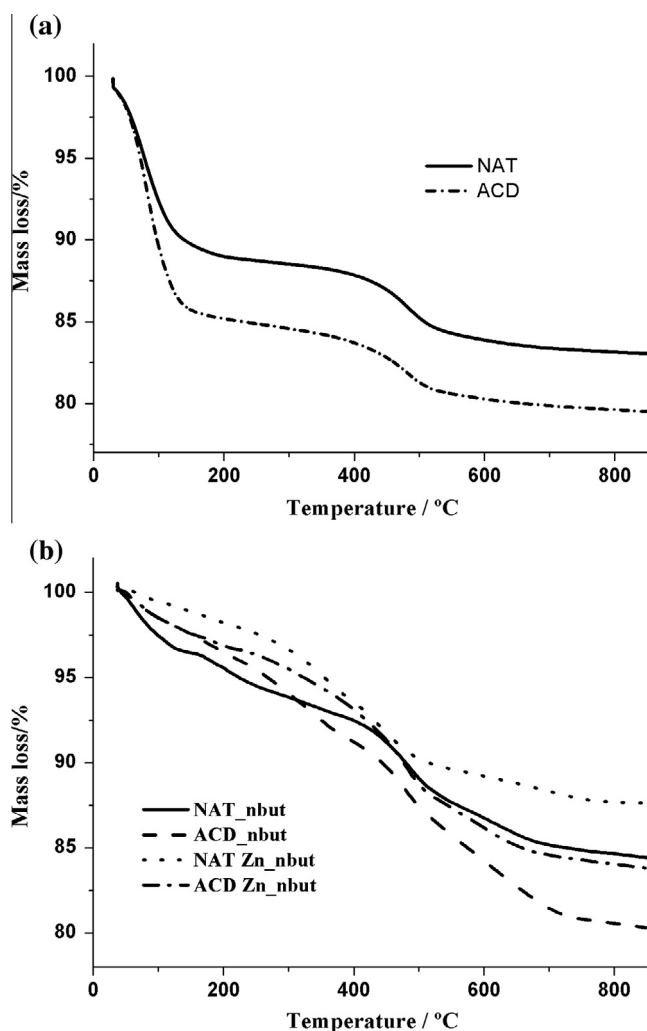
Fig. 3. Thermogravimetric curves of (a) NAT and ACD clays before n-butylamine adsorption; (b) NAT, ACD, NAT Zn and ACD Zn samples after n-butylamine adsorption.

performed on natural bentonite, deposition on the clay particles occurred. These depositions were not homogeneous, with formation of agglomerated material with a brighter color on the surface of darker particles. The most homogeneous impregnation took place for ZnO on the natural clay (NAT Zn).

In relation to the surface area, the results presented in Table 1 indicate that acid treatment led to a significant decrease in the surface area. This behavior can be explained by the removal of impurities with small particle sizes during acid treatment. Impregnation of the oxides on the natural clay leads to an 18% increase in the surface area for NAT Zn and a 122% increase for NAT Ce. For samples prepared using the acid clay, this increase was remarkable for all oxides with an increase larger than 250%. This behavior is related to a nonhomogeneous deposition of the oxides on the surface of the bentonite and to a segregation of the oxides, particularly for the acid clays, as shown in the FE-SEM micrographs.

The use of n-butylamine as probe molecule for determination of acid properties is well known in literature [22,28–29]. For instance, Ruiz et al. [29] evaluated the acid sites of palygorskite clays by the mass loss of adsorbed n-butylamine, evaluated by thermogravimetric analysis. This work was used as reference for the correlation among mass loss regions in the thermogravimetric curves with the acid strength sites identified by n-butylamine thermosorption. According to the authors, four mass loss regions were identified: the first one was assigned to n-butylamine physical adsorption with mass loss between 27 and 110 °C; the second one was related to a weak chemisorption in the temperature range from 110 to 210 °C; in the third one, medium chemisorption was quantified between 210 and 330 °C; the fourth mass loss in the range from 330 to 720 °C was assigned to strong chemisorption. According to Silva et al. [22], the physisorbed n-butylamine is related to very weak acid sites, which do not contribute effectively to chemisorption phenomena at low temperatures.

The thermogravimetric curves obtained in the present work for samples NAT, ACD, NAT Zn and ACD Zn are presented in Fig. 3. Quantification of n-butylamine desorption from the different acid strength sites are indicated in Table 2, as well as the temperature range of n-butylamine mass losses. The acidity calculation considered a 1:1 adsorption stoichiometry, similarly to Ruiz et all [29], while the total acidity was calculated by the sum of n-butylamine mass loss considering only chemisorption which is related to weak, medium and strong acid sites.

3.2. Catalytic test

The results for the viscosity of the oils after the catalytic test are shown in Table 3. Lower viscosities were obtained for the samples catalyzed by ACD, NAT Zn and NAT Ce, which indicates that these materials have a higher activity. Impregnation of the oxides on the acid clay leads to a reduction in activity.

Table 2
Adsorption site distribution for NAT, ACD, NAT Zn and ACD Zn.

Sample	Acidity (mmol g^{-1})	Adsorption type	Desorption range, ΔT (°C)	Total acidity (mmol g^{-1})
NAT	1.65	Physical adsorption	30–144	0.43
	0.21	Weak chemisorption	144–291	
	0.16	Medium chemisorption	291–380	
	0.06	Strong chemisorption	380–790	
NAT Zn	0.09	Physical adsorption	61–104	1.15
	0.25	Weak chemisorption	104–226	
	0.66	Medium chemisorption	226–395	
	0.24	Strong chemisorption	395–865	
ACD	0.27	Physical adsorption	47–106	2.31
	0.40	Weak chemisorption	106–221	
	0.80	Medium chemisorption	221–396	
	0.64	Strong chemisorption	396–780	
ACD Zn	0.40	Physical adsorption	47–154	1.48
	0.13	Weak chemisorption	154–217	
	0.40	Medium chemisorption	217–357	
	0.95	Strong chemisorption	357–732	

Table 3
Viscosity values of the oil after the catalytic tests.

Catalyst	Viscosity ($m^2\ s^{-1}$)	Reduction (%)	Catalyst	Viscosity ($m^2\ s^{-1}$)	Reduction (%)
Soybean oil	34.0	0	Soybean oil	34.0	0
ACD – 1 h	18.3	46.2	NAT – 1 h	32.0	5.9
ACD – 2 h	16.1	52.6	NAT – 2 h	26.4	22.3
ACD – 4 h	12.7	62.6	NAT – 4 h	31.2	8.2
ACD Cu – 1 h	30.9	9.1	NAT Cu – 1 h	32.8	3.5
ACD Cu – 2 h	29.5	13.2	NAT Cu – 2 h	32.8	3.5
ACD Cu – 4 h	27.3	19.7	NAT Cu – 4 h	31.3	7.9
ACD Zn – 1 h	29.3	13.8	NAT Zn – 1 h	26.2	22.9
ACD Zn – 2 h	26.2	22.9	NAT Zn – 2 h	16.0	52.9
ACD Zn – 4 h	21.1	37.9	NAT Zn – 4 h	8.4	75.3
ACD Ce – 1 h	35.5	0	NAT Ce – 1 h	33.2	2.3
ACD Ce – 2 h	32.4	4.7	NAT Ce – 2 h	28.2	17.6
ACD Ce – 4 h	26.4	22.3	NAT Ce – 4 h	16.2	52.3

Results described in Table 2 indicate that acidification of NAT clay and ZnO impregnation onto ACD clay lead to significant variation of the amount of the different acid sites as well as to a significant variation of the total acidity of these catalysts. In relation to the acidification process, a high efficiency is attained with a 5-fold increase of the total acidity for ACD clay comparing to NAT one. While the amount of very weak acid sites (which do not contribute to the catalytic process) had a significant decrease, the amount of weak, medium and strong acid sites were increased by 2, 5 and 11 times, respectively. For ZnO impregnation onto the NAT Clay (NAT Zn), a 3-fold increase of the total acidity was attained. Once again a significant decrease of the very weak acid sites was observed, besides a 4-fold increase of the medium and strong acid sites. The same behavior was not observed for ZnO impregnation onto ACD clay (ACD Zn). For this sample, the total acidity was reduced to half comparing to ACD, indicating that the alkaline conditions used in the impregnation process are not adequate for acid clays. For ACD Zn, only the amount of very weak acid sites and of strong acid sites increased, while the amount of weak and medium acid sites decreased 3 and 2 times, respectively.

These results confirm that a change in the characteristics of the acidic clay takes place due to the hydrothermal/solvothermal synthesis in alkaline medium, which reduces the acid sites of the bentonite. Moreover, this reduction in activity after impregnation of acidic clay can also be related to the distribution of the metal oxide on the ceramic particles because clays with acid treatment led to the impregnation of agglomerates both on the surface of and outside the interlamellar region (Fig. 2), whereas impregnations on the natural clays caused a coating to form around the clay particles. This behavior may contribute to a larger dispersion of oxides on the clay, leading to the exposition of more active sites for the NAT Ce and NAT Zn samples. The activity of the ACD sample may be related to the presence of acid groups on the surface acting as active sites that promote the transesterification reaction in spite of the low surface area of this material compared with the NAT sample.

The reduction in viscosity of the oils likely indicates that transesterification occurred. This reduction takes place even when the reaction is not complete and diacylglycerides or monoacylglycerides are still present in the material.

^{1}H NMR spectroscopy was used for a better evaluation of the reaction (Fig. 4). The region of the spectrum between 0 and 3.0 ppm is characteristic of peaks assigned to the fatty acid groups constituting triglycerides, which do not change after transesterification [30,31]. The transesterification reaction can be evaluated by considering the two doublet of doublets between 4.0 and 4.4 ppm and the 5.2 ppm peak associated with the hydrogens of the CH_2 and CH groups present in the triglycerides, respectively [23,24],

which are modified after the reaction. According to the reaction mechanism, mono- and diacylglycerides are intermediates in the transesterification reaction, and these peaks disappear if the reaction is complete. Moreover, the production of ethyl esters can be shown by the quartet between 4.0 ppm and 4.2 ppm, characteristic of etoxila methyl groups originally present in the ethyl alcohol [23,24].

The behavior observed in the ^{1}H NMR spectra of glycerides may be analyzed by considering the structures of the different acylglycerol classes (MAG – monoacylglycerides, DAG – diacylglycerides or TAG – triacylglycerides) and the fatty acid ethyl esters (FAEE). These structures are represented in the inset of Fig. 4a [31].

The ^{1}H NMR spectra of the samples after the catalytic tests are presented in Fig. 4a. It is possible that FAEE formation is negligible for NAT-, NAT Cu- and ACD Cu-catalyzed samples because the profiles of their ^{1}H NMR spectra are very similar to that of the oil (Fig. 4b), whereas the peaks assigned to FAEE, between 4.0 and 4.2, are not observed. These samples also showed less reduction in their viscosity values and approached the results obtained for the oil.

The oils catalyzed with NAT Ce, ACD Ce and ACD Zn samples show an overlap of the doublet of doublets and the quartet that is observed between 4.0 and 4.2 ppm. Moreover, the ^{1}H NMR spectra for the samples catalyzed by these materials also indicate the presence of TAG and the formation of FAEE, 1,2-DAG and MAG-1. This result indicates that the conversion of TAG into ethyl esters was incomplete [23,24].

The spectra of samples obtained with ACD and NAT Zn show a significant decrease in the doublet of doublets in the region between 4.2 and 4.4 ppm and the appearance of a quartet between 4.0 and 4.2 (Fig. 4b). These samples exhibit ^{1}H NMR spectra characteristic of a large amount of FAEE from the presence of protons b and an almost insignificant amount of $\alpha_{1,2}$ and α_1 protons (characteristic of 1,2-DAG and 1-MAG), especially for the sample catalyzed by NAT Zn, indicating that this catalyst led to a better performance than ACD. It is important to emphasize that these samples also showed the largest reduction in viscosity values.

Several studies have reported the use of ^{1}H NMR spectroscopy to quantify the conversion of oils into fatty acid esters [23–25,30,32–33]. Ghesti [24] and Costa-Neto [25] reported the use of this technique for transesterification reactions using ethyl alcohol. The conversion values obtained in this study (Table 4) are consistent with the reduction in viscosity, and the peaks present in the ^{1}H NMR spectra confirm that the use of ACD, NAT Ce, and NAT Zn catalysts leads to larger conversions, whereas lower conversions were obtained with NAT Cu, ACD Cu and NAT catalysts. Though they were used to evaluate the conversion, superposition of the peaks assigned to tri-, di- and
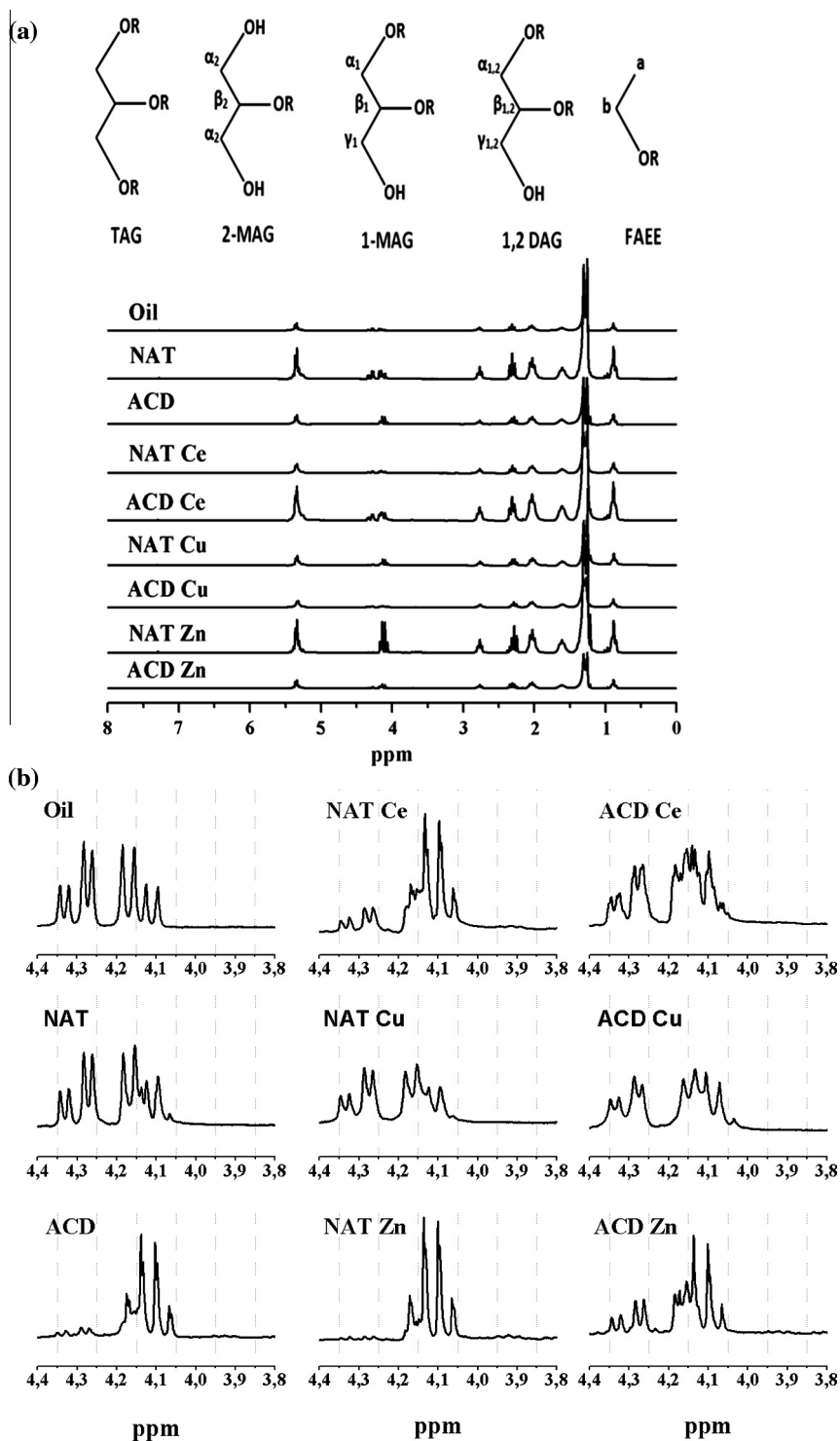
Fig. 4. (a) ^{1}H NMR spectra of soybean oil and of the products obtained after the catalytic tests. Inset: Structures of the MAG – Monoacylglycerol, DAG – Diacylglycerol, TAG – Triacylglycerol and FAEE – fatty acid ethyl ester [34]; (b) amplification of the ^{1}H NMR spectra between 3.8 and 4.4 ppm.

Table 4
Conversion percentages (C_{EE}) obtained after catalytic tests.

Samples	Oil	NAT Cu	ACD Cu	NAT	ACD Ce	ACD Zn	ACD	NAT Ce	NAT Zn	Biodiesel
% C_{EE}	0[a]	11.0	13.5	15.5	25.5	40.0	55.0	75.0	88.0	100[a]

[a] The values of 0% and 100% were attributed to pure soybean oil and pure ethyl esters, respectively.

monoacylglycerides in the ^{1}H NMR spectra do not permit one to evaluate which reactions are not complete and which intermediates (such as di- and monoacylglycerides) are present.

The characterization of these intermediates was carried out by ^{13}C NMR spectroscopy, as shown in the spectra of the samples before and after 4 h of catalytic tests (Fig. 5a). In the ^{13}C NMR spectra, the transesterification reaction can be confirmed by the chemical shift of the signals between 56 and 70 ppm (highlighted region in Fig. 5b). In this case, a reduction in the signals assigned to the methylene group of the glycerol is observed at 62 and 69 ppm, whereas another signal appears at 60 ppm, which is assigned to the ethylene group of the alcohol moiety of the ester group [CH$_3$CH$_2$OC(=O)—R]. The presence of residual mono-, di- and triglycerides can also be identified in the ^{13}C NMR spectra based on the data presented in Table 5 [23,34–35].

A closer look at the region between 56 and 70 ppm, as presented in Fig. 5b, shows important differences after the catalytic tests. The spectra of the samples after reaction in the presence of NAT Cu and NAT catalysts are very similar to the oil before transesterification, without peaks assigned to esters, mono- or diacylglycerides, indicating that almost no conversion occurred with these catalysts. According to the spectra obtained for the samples catalyzed by NAT Ce, ACD Ce, ACD Cu and ACD Zn, peaks characteristic of ethyl esters are observed at 60 ppm, but it is also possible to observe the formation of diacylglycerides and small amounts of monoacylglycerides, in addition to the presence of residual triacylglycerides, which indicates the ineffectiveness of these catalysts for complete conversion to the ethyl esters.

The samples obtained with ACD and NAT Zn catalysts have more noticeable differences. In these spectra, a significant reduction of the peak at 62 ppm and the disappearance of the peak at 69 ppm are observed, and another high-intensity peak appears at 60 ppm. These peaks indicate that only small amounts of mono-, di- and triacylglycerides are still present in these samples.

Among all of the tested catalysts, the sample catalyzed by NAT Zn presented the largest conversion, as indicated by the lowest viscosity values, by the NMR spectra (^{1}H- and ^{13}C) and by conversion calculations, which indicate that a large amount of FAEE was formed. The catalytic activity of the NAT Zn catalyst is directly related to a better dispersion of the active phase on the support, as indicated in the FE-SEM results, whereas no correlation with surface area was observed. In other words, the metal oxide must be
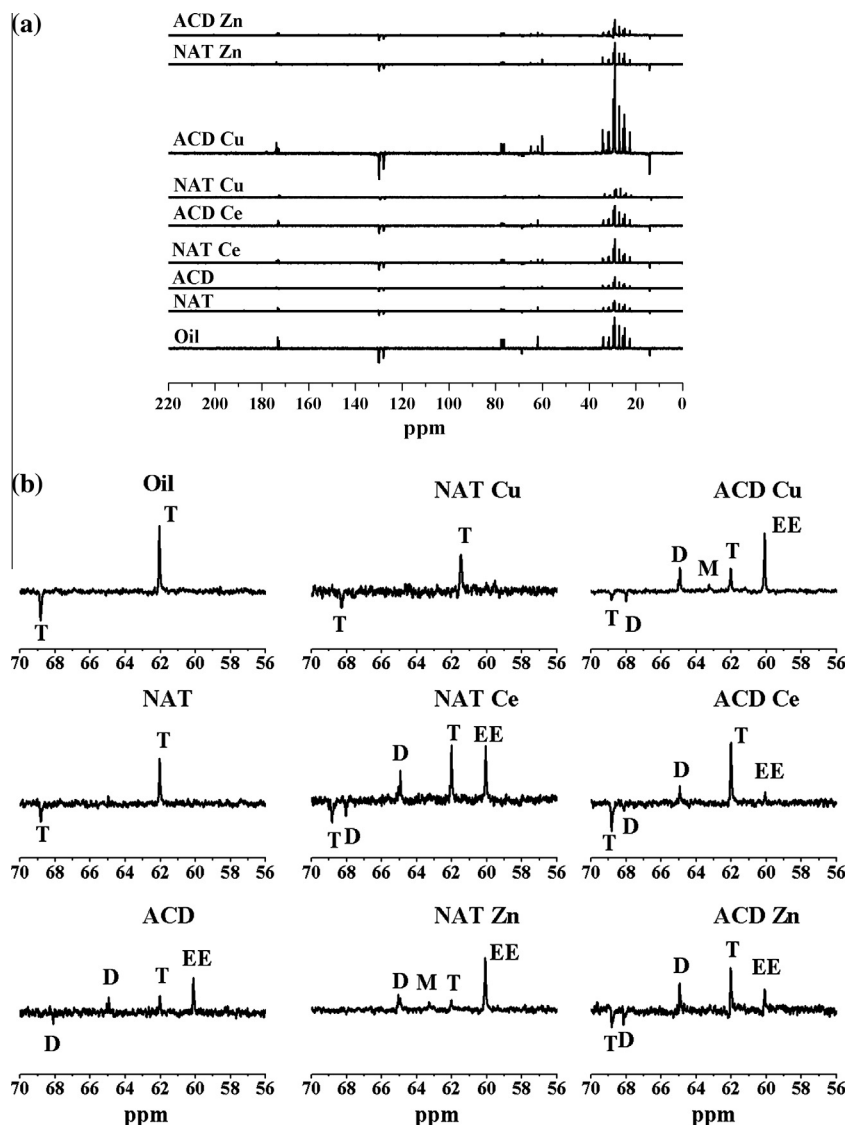

Fig. 5. (a) ^{13}C NMR spectra of the samples after catalytic test; (b) amplification of the spectra between 56 and 70 ppm. Assignments were done in agreement to Table 5; M = monoacylglycerol, D = diacylglycerol, T = triacylglycerol and EE = ethyl ester.

Table 5
Chemical shift values (δ) of carbons in different classes of glycerides and in ethylic ester [36–37].

Resonance code	δ (ppm)	Carbon atom
D; T	62.04	$-CH_2$/sn-1,2-Diacylglycerides; $-CH_2$/Triacylglycerides
M	63.34	$-CH_2$/sn-1-Monoacylglycerides
D	64.99	$-CH_2$/sn-1,2-Diacylglycerides
D	68.14	$-CH$/sn-1,3-Diacylglycerides
T	69.02	$-CH$/Triacylglycerides
M	70.37	$-CH$/sn-1-Monoacylglycerides
EE	60.00	($-CH_2-CH_3$) – Ethylene group of the alcohol moiety of the ester

homogeneously distributed over the bentonite surface. Moreover, the choice of the appropriate clay is extremely important to obtain a better interaction between the catalyst and the support.

In spite of the larger conversion into ethylic esters (Table 4), NAT Zn has a smaller total acidity than ACD and ACD Zn. This behavior may be related to the different acid strength sites present in each material. BONELLI et al. [38] evaluated the influence of the catalyst superficial acidity on the transesterification reaction using homogeneous and heterogeneous catalysts. The authors found out that an optimal range of strength for Lewis acidic catalysts exists, as strong acid sites seem to be less active for transesterification reactions because desorption of reaction products is unfavorable, making subsequent reactions more difficult. In the present work, ACD and ACD Zn have a high total acidity but 28% and 64% of these sites are assigned to strong ones, respectively. As a consequence, a smaller conversion takes place, especially for ACD Zn leading to the presence of triacylglycerides even after 4 h of reaction.

For NAT Zn, ZnO impregnation increases the catalytic activity with a significant increase in the amount of medium acid sites comparing to the NAT clay. According to literature, ZnO has an amphoteric character with a high efficiency in transesterification of oils even in the presence of high amount of free fat acids. Triacylglyceride molecules adsorb on the Zn^{2+} sites on the surface, behaving as Lewis acid, while O^{2-} sites behave as Lewis base favoring methanol adsorption to promote the transesterification reaction [10].

The transesterification reaction was evaluated by gas chromatography for the sample obtained with the NAT Zn catalyst. According to the chromatogram, a 82.1 ± 0.5% conversion of fatty acid ethyl esters was achieved, similar to the value obtained by ^{1}H NMR (88.0%). These results confirm that the catalyst system composed of bentonite impregnated with ZnO is an interesting alternative for biodiesel synthesis.

4. Conclusions

The microwave-assisted hydro/solvothermal method was effective in the synthesis of the catalysts, leading to a substantial change in the characteristics of the clay. The impregnation of oxides using acid bentonite as a support led to the formation of agglomerated particles but that a larger dispersion was attained for the natural clay.

The largest viscosity reduction after catalytic tests and the largest ester conversion were obtained for NAT Zn, which presented a large dispersion on the bentonite surface during impregnation with higher amount of medium acid sites, and for ACD, which contains weak and medium acid groups that are active in the catalysis. The natural bentonite (NAT) was not catalytically active for biodiesel synthesis but can be used as a support.

Acknowledgements

References

[1] Karmee SK, Chadha A. Preparation of biodiesel from crude oil of Pongamia pinnata. Bioresour Technol 2005;96:1425–9.

[2] Vaccari A. Clays and catalysis: a promising future. Appl Clay Sci 1999;14:161–98.

[3] Meille V. Review on methods to deposit catalyts on structured surfaces. Appl Catal A: Gen 2006;315:1–17.

[4] Klingshirn CF. ZnO: material, physics and applications. Chem Phys Chem 2007;8:782–803.

[5] Minsoo K, Lee H, Yoo SJ, Youn YS, Shin YH, Lee YW. Simultaneous synthesis of biodiesel and zinc oxide nanoparticles using supercritical methanol. Fuel 2013;109:279–84.

[6] Zieba A, Pacuła A, Serwicka EM, Drelinkiewicz A. Transesterification of triglycerides with methanol over thermally treated $Zn_5(OH)_8(NO_3)_2$ $2H_2O$ salt. Fuel 2010;89:1961–72.

[7] Newman SP, Jones W. Comparative study of some layered hydroxide salts containing exchangeable interlayer anions. J Solid State Chem 1999;148:26–40.

[8] Lukic I, Kesic Z, Maksimovic S, Zdujic M, Liu H, Krstic J, et al. Kinetics of sunflower and used vegetable oil methanolysis catalyzed by CaO_ZnO. Fuel 2013;113:367–78.

[9] Yan S, Mohan S, DiMaggio C, Kim M, Simon Ng KY, Salley SO. Long term activity of modified ZnO nanoparticles for transesterification. Fuel 2010;89:2844–52.

[10] Yan S, Salley SO, Simon Ng KY. Simultaneous transesterification and esterification of unrefined or waste oils over ZnO–La$_2$O$_3$ catalysts. Appl Catal A: Gen 2009;353:203–12.

[11] Corro G, Pal U, Tellez N. Biodiesel production from Jatropha curcas crude oil using ZnO/SiO$_2$ photocatalyst for free fatty acids esterification. Appl Catal B: Environ 2013;129:39–47.

[12] Mguni LL, Mukenga M, Muzenda E, Jalama K, Meijboom R. Expanding the synthesis of Stöber spheres: towards the synthesis of nano-magnesium oxide and nano-zinc oxide. J Sol–Gel Sci Technol 2013;66:91–9.

[13] Hussain ST, Ahmed W, Saeed M, Ali SD, Asma M. Fatty acid methyl ester production from waste cooking oil catalyzed by CuO–CeO$_2$/NiO mixed oxides. J Renew Sustain Energy 2013;5:023104–23112.

[14] de Caland LB, Santos LSS, de Moura CVR, de Moura EM. Preparation and study of bimetallic compounds efficiency in the synthesis of biodiesel fuel. Catal Lett 2009;128:392–400.

[15] Yang R, Su M, Li M, Zhang J, Hao X, Zhang H. One-pot process combining transesterification and selective hydrogenation for biodiesel production from starting material of high degree of unsaturation. Bioresour Technol 2010;101:5903–9.

[16] Thitsartarn W, Kawi S. An active and stable CaO–CeO$_2$ catalyst for transesterification of oil to biodiesel. Green Chem 2011;13:3423–30.

[17] Kawashima A, Matsubara K, Honda K. Development of heterogeneous base catalysts for biodiesel production. Bioresour Technol 2008;99:3439–43.

[18] Ramírez MM, Gómez R, Cortez JGH, Moreno AZ, Germán CMRS, Valle SOF. Advances in the transesterification of triglycerides to biodiesel using MgO–NaOH, MgO–KOH and MgO–CeO$_2$ as solid basic catalysts. Catal Today 2013;212:23–30.

[19] Kim M, DiMaggio C, Yan S, Salley SO. Simon Ng KY, The effect of support material on the transesterification activity of CaO–La$_2$O$_3$ and CaO–CeO$_2$ supported catalysts. Green Chem 2011;13:334–9.

[20] Yu X, Wen Z, Li H, Tu ST, Yan J. Transesterification of Pistacia chinensis oil for biodiesel catalyzed by CaO–CeO$_2$ mixed oxides. Fuel 2011;90:1868–74.

[21] Hassan JJ, Hassan Z, Hassan HA. High-quality vertically aligned ZnO nanorods synthesized by microwave-assisted CBD with ZnO–PVA complex seed layer on Si substrates. J Alloys Compd 2011;509:6711–9.

[22] Silva AOS, Souza MJB, Aquino JMFB, Fernandes Jr VJ, Araujo AS. Acid Properties of the HZSM-12 zeolite with different Si/Al ratio by thermo-programmed desorption. J Therm Anal Calorim 2004;76. 783-79.

[23] Fatimah I, Wang S, Wulandari D. ZnO/montmorillonite for photocatalytic and photochemical degradation of methylene blue. Appl Clay Sci 2011;53:553–60.

[24] Lopez JM, Cota TNJG, Monterrosas EEG, Martínez RN, de la Cruz González VM, Flores JLA, Ortega YR. Kinetic study by ^{1}H nuclear magnetic resonance spectroscopy for biodiesel production from castor oil. Chem Eng J 2011;178:391–7.

[25] Compton DL, Laszlo JA, Appell M, Vermillion KE, Evans KO. Synthesis, purification, and acyl migration kinetics of 2-monoricinoleoylglycerol. J Am Oil Chem Soc 2014;91:271–9.

[26] Mishra BG, Rao GR. Cerium containing Al- and Zr-Pillared clays: promoting effect of cerium (III) ions on structural and catalytic properties. J Porous Mater 2005;12:171–81.

[27] Frenkel M. Surface acidity of montmorillonites. Clays Clay Miner 1974;22:435–41.

[28] Ruiz AC, Melo DMA, Souza JR, Alcazar LO. Determination of total acid in palygorskite chemically modified by n-butylamine thermodesorption. Mater Res 2002;5:173–8.

[29] Guzatto R, Defferrari D, Reiznautt QB, Cadore ÍR, Samios D. Transesterification double step process modification for ethyl ester biodiesel production from vegetable and waste oils. Fuel 2012;92:197–203.

[30] Ghesti GF, de Macedo JL, Resck IS, Dias JA, Dias SCL. FT-Raman spectroscopy quantification of biodiesel in a progressive soybean oil transesterification reaction and Its correlation with ^{1}H NMR spectroscopy methods. Energy Fuels 2007;21(5):2475–80.

[31] Neto PRC, Caro MSB, Mazzuco LM, Nascimento MdaG. Quantification of soybean oil ethanolysis with ^{1}H NMR. J Am Oil Chem Soc 2004;81(12):1111–4.

[32] Gelbard GBO, Vargas RM, Vielfaure F, Schuchardt UF. [1]H nuclear magnetic resonance determination of the yield of the transesterification of rapeseed oil with methanol. J Am Oil Chem Soc 1995;72(10):1239–41.

[33] Monteiro MR, Ambrozin ARP, Liao LM, Ferreira AG. Determination of biodiesel blend levels in different diesel samples by ^{1}H NMR. Fuel 2009;88:691–6.

[34] Casas A, Ramos MJ, Pérez A, Símon A, Torres CL, Moreno A. Rapid quantitative determination by ^{13}C NMR of the composition of acetylglycerol mixtures as byproduct in biodiesel synthesis. Fuel 2012;92:180–6.

[35] Moreira ABR, Perez VH, Zanin GM, de Castro HF. Biodiesel synthesis by enzymatic transesterification of palm oil with ethanol using lipases from several sources immobilized on silica–PVA composite. Energy Fuels 2007;21:3689–94.

[36] Siddiqui N, Sim J, Silwood CJL, Toms H, Iles RA, Grootveld M. Multicomponent analysis of encapsulated marine oil supplements using high-resolution ^{1}H and ^{13}C NMR techniques. J Lipid Res 2003;44:2406–27.

[37] Fernandes JLN, de Souza ROMA, Azeredo RBV. ^{13}C NMR quantification of mono and diacylglycerols obtained through the solvent-free lipase-catalyzed esterification of saturated fatty acids. Magn Reson Chem 2012;50:424–8.

[38] Bonelli B, Cozzolino M, Tesser R, Di Serio M, Piumetti M, Garrone E. Study of the surface acidity of TiO_2/SiO_2 catalysts by means of FTIR measurements of CO and NH_3 adsorption. J Catal 2007;246:293–300.